VOL. 17, NO. 19, OCTOBER 2022 ISSN 1819-6608
ARPN Journal of Engineering and Applied Sciences

www.arpnjournals.com

EVALUATION OF SHEAR STRENGTH PARAMETERS AND DEFORMABILITY OF MARLEY FORMATION IN AMMAN

Khair Al-Deen Bsisu and Wassel Al-Bodour
Department of Civil Engineering, School of Engineering, The University of Jordan, Jordan
E-Mail: k.bsisu@ju.edu.jo

ABSTRACT

Marl is a general term that refers to any material, whether soil or rock-like, that contains 35-65 percent calcium carbonate and the rest of clay fraction (Al-Amoudi *et al*., 2010; Yong & Ouhadi, 2007) this formation is a rock-like when dry, never the less, it is a soft soil-like when moist. In general, high deformation and settlement are the main problems of Marl. In Amman-Jordan, the seasonal variations of water contents is the primary cause of deformability and failure problems of Marls. Mainly because most of the geotechnical studies are performed during the dry seasons, during which Marls show enhanced engineering properties. During the wet seasons, water percolates and all mechanical properties drastically deteriorate. Accordingly, several failures and excessive deformation incidents take place due to these seasonal cycles of wetting and drying. This research work is intended to investigate the mechanical properties of Amman Marls in a manner that enables overcoming the problems originated from the wetting seasonal variations, and the difficulty of obtaining intact samples that may reasonably represents the realistic conditions and properties of this formation Most of the formation in Amman consist of limestone and Marl. Marl a top soil strata in several parts in Amman is exposed to changing weather conditions of wetting and drying in the Greater Amman area. The bearing capacity of Marl is not consistent, and cannot be simply estimated when it is essentially changing in relation to its water content. In this study, deformability and strength characteristics of Marl are investigated by performing a series of field and laboratory tests including drilling and sampling, plate load test (PLT), unconfined compressive strength (UCS) test, seismic refraction and tomography (SRT), and multi-channel analysis of surface waves (MASW).

Keywords: bearing capacity, marl, plate load test, seismic refraction and tomography, unconfined compressive strength.

INTRODUCTION

Many buildings and structures that were constructed on these types of soil have been damaged in various countries, in spite of the adequate design of the structure and foundation. This is due to the lack of precise and reliable determination of strength and the worst case expected maximum deformation (Akili & Torrance, 1981; Hooshmand *et al*., 2012; Milani *et al*., 2017).

Marl is a swelling soil that gives a significant increase in volume when the water content is increased and shrinks and cracks are formed when the water content is decreased (Arifuzzaman *et al.*, 2017). The amount of swell and shrinkage is influenced by a number of factors such as soil structure, amount and type of clay minerals in the soil, confining pressure, void ratio, climate changes, and initial moisture content (Firoozi *et al.*, 2017; Salimi *et al.*, 2018). The clay mineral constituents of Marl, palygorskite; a magnesium aluminium phyllosilicate with the chemical formula (Mg,Al) 2Si 4O 10(OH)·4(H 2O) and sepiolite; a fibrous hydrated magnesium silicate with the chemical formula Mg 4Si 6O 15(OH)2·6H2O, leading to instability of such soils(Benyahia *et al*., 2020; Lamas *et al*., 2002). Swell-shrink soils have low strength and high plasticity, causing instability in lightly loaded structures (Jalal *et al*., 2021). Saturated Marls and saturated or semi-saturated clayey soils, have a low permeability coefficient, consolidation and void ratio reduction take time, therefore settlement prediction and duration are critical for construction works (Milani *et al.*, 2017).

Several studies have been conducted to characterize Marls and their geotechnical and engineering properties. Amiri *et al.* (2022) studied the effects of lead contaminants on engineering properties of Iranian Marl soil from the microstructural perspective. This was performed by artificial contaminating of Marl soil with varying lead concentrations and measurement of some geo-environmental (pH, cation exchange capacity (CEC), and contaminant retention) and geotechnical (Atterberg limits, compressive strength, granularity, and permeability) characteristics. Changes in mineralogy and microstructural behavior of lead-contaminated soil were also investigated using X-ray diffraction (XRD) patterns and scanning electron microscope (SEM) images.

Vakili *et al.* (2021) studied the application of the dynamic cone penetrometer test for determining the geotechnical characteristics of Marl soils treated by lime. An attempt was made to provide a correlation between UCS, California bearing ratio (CBR), subgrade reaction coefficient (K_s) and dynamic penetrometer index (DPI) parameters.

Hooshmand *et al*. (2012) studied the mechanical and physical characterization of Tabriz Marls, Iran. In the Tabriz area (Iran), three types of Marls can be found: green, yellow, and grey/black Marls. Various in situ and laboratory tests are used to investigate the strength and deformation characteristics of Tabriz Marls and their stress-strain behavior. Test results showed that the deformation modulus values obtained from the pressure meter test was in good agreement with those obtained from the PLT. As a result, the pressure meter test is a good in-situ technique for evaluating the deformation modulus of Marly formations. Deformation modulus obtained from seismic wave test was approximately 30–50 times the

static deformation modulus and the deformation modulus obtained from pressure meter and plate loading tests were about 4-5 times the results of uniaxial compressive test. Stress-strain curves showed that the minimum value of strain and the maximum value of strength and deformation modulus are corresponding to the grey/black Marls while the maximum value of strain at the elastic and failure points and the minimum value of strength and deformation modulus are corresponding to the yellow Marls. Between different characteristics of Tabriz Marls, some empirical relationships were also discovered.

Shaqour *et al.* (2008) studied the geotechnical and mineralogical characteristics of Marl deposits in Jordan. Representative samples of Marl horizons were tested for mineral composition, and for a set of index and geotechnical properties including: Atterberg limits, specific gravity, grain size, Proctor compaction, and shear strength properties, using X-ray diffraction technique along with chemical analysis. The results reveal that a positive linear relationship between the liquid-plastic boundary and the clay content. In both standard and modified compaction, tests results show an inverse linear relationship between the maximum dry density and the clay content. Water adsorption by clay minerals is attributed for this. Moreover, the results show that the angle of internal friction has a similar relationship. There was no clear correlation between cohesion and clay content.

PLT is used to determine the vertical deformation and strength properties of soil by measuring the variations of applied force versus plate penetration. It can be used for determining a number of ground parameters such as: modulus of subgrade reaction, elastic modulus, settlement behavior, and allowable bearing pressure(Anyang et al., 2018).

UCS testis used to determine compressive strength of rock specimens under uniaxial loading (Nazir *et al.*, 2013). In this test method, the UCS is taken as the load per unit area at 15% axial strain, or the maximum load attained per unit area if stress strain peak is manifested, whichever occurs first during the performance of a test (Ige & Ajamu, 2015). Besides UCS, this test can be used to determine several important parameters related to rock deformation, including unconfined Young's modulus, Poisson's ratio, and failure and ultimate or peak stresses along with corresponding strains (Nazir *et al.*, 2013).

Seismic refraction is a geophysical technique that is commonly used to investigate subsurface layers and/or local anomalies. This technique is widely employed in a variety of fields, including engineering, groundwater, environmental, hydrocarbons, and industrial-mineral exploration (Hodgkinson & Brown, 2005; Khalil & Hanafy, 2008; Lankston, 1989). The seismic refraction technique relies on measuring the travel time of primary seismic waves refracted at the interfaces between subsurface layers of different velocities (Anomohanran, 2013; Ayolabi *et al.,* 2009). The inability to detect or recognize the existence of certain layers, referred to as hidden layers or blind zones, is one of the seismic refraction's limitations. This is due to insufficient velocity contrast of layer thickness(Bery, 2013).

SRT is a geophysical method of interpreting seismic refraction data which uses a gridded inversion technique to determine the velocity of two-dimensional and three-dimensional models (Al-Saigh & Al-Heety, 2014). The aim of this method is to detect the subsurface layers using a primary wave velocity (Vp) as a 2-D cross-section (Ghanem *et al.*, 2021).

MASW is a non-destructive seismic method to determine shear wave velocity (Vs) and thickness of the soil column (Mahajan *et al.*, 2007). The dispersive phase velocity of the surface Rayleigh waves is inverted to obtain vertical shear-wave velocity profiles (Cichowicz *et al.*, 2011).

The main purpose of this study to develop an integrated framework to evaluate deformability and strength of the Marly formations in Amman. The following tasks were carried out to achieve the objective of the study:

a) Geotechnical exploration to assess the soil profile by drilled borehole and MASW.

b) Geotechnical Characterization of Marlusing PLT, UCS test, SRT, and MASW.

c) Combining the results of SRT, MASW, and borehole lithology to delineate the shallow subsurface layers.

d) Investigating the bearing capacity of Marlin Amman.

e) Deformability parameters of Marl formations in Amman.

The study's significance is in determining an approach to evaluating soil parameters using PLT, UCS test, SRT, and MASW. Because Marl appears as a rock in dry conditions but becomes clay in wet conditions, obtaining samples in any circumstance is extremely difficult.

METHODOLOGY

Primarily, Amman Marls in its normal conditions are not saturated or at least the water content is not influential within such given conditions. Correspondingly, structures founded on Marls experience no problems during the normal conditions. However, extreme wetting season every few years is not unusual in Amman. Upon the recurrence of the extreme wetting, Marl characteristics experience drastic changes that becomes the controlling aspect of the mechanical behavior of Marl as a foundation. Unless these scenarios of exposure are not addressed during the exploration, design, construction, and operation stages, critical problems might be encountered.

On the other hand, retrieving intact samples, within the normal condition is Amman, is not a rule of thumb. High and expensive technologies are required to collect enough number of intact samples, performing

representative tests (like triaxial), soaking and saturation, and eventually to pick the proper formulation for strength and deformability. Most of the available formulae are for rock or soils which might not be necessary correct for the Marl formation. Using these formulations with the mechanical properties of Marl might be either costly safe, or critical unsafe.

Accordingly, this research work has been undertaken to evaluate strength and deformability parameters, and the practical techniques and methods that allow measurements and interpretation in reasonable and effective way that can be used for geotechnical studies, such as; bearing capacity calculations, settlement evaluation, and stability checks for foundations on the Marl formations in Amman. The sought parameters to be calibrated based on the PLT test, seismic refraction, and the UCS test for both wet and dry samples.

The research work is handled through field and lab testing. The laboratory testing was intended to evaluate the Marl index parameters like the density, moisture content, UCS. The field testing consists of two different methodical approaches, the plate load test and the seismic wave methods. Indirect interpretations for the required parameters using the embedded inter relations between the field testing and the lab and field tests. Procedures and correlations were developed for deformability and strength and provided as well. The study was performed according to the following procedure:

a) Five representative sites, that contains large amount of Marls, were selected such that they cover the major areas of Amman city.
b) Two boreholes were drilled in each site. Cores and intact samples were collected for the later use in lab testing. Primarily, water content, unit weight, and the uniaxial strength test obtained from the laboratory testing
c) Immediately after drilling and sampling operations were completed the plate load tests were conducted for two conditions
a. Natural conditions (during the dry season)
b. Wet condition up 5-hour wetting cycles (please correct me if I am wrong)

d) The geophysical MASW had been conducted after the PLT tests were completed (please correct me if I am wrong)

The interpretation of the field measurements and lab test results were conducted according to following:

a) Unconfined elastic modulus, unit weight, and water content were obtained from the collected samples in the laboratory
b) The plate load testing results were interpreted to obtain the ultimate capacity and the modulus of subgrade from the test results based on the raw data
c) The PLT results were interpreted in another layer of computations to obtain the elastic modulus of the layer within the bearing failure mechanism below the plate
d) The PLT ultimate capacity were used to back analyze, the shear strength parameters for Terzagli's bearing capacity. The analysis had taken into consideration the short term condition (wet undrained) and the long term condition (dry condition)
e) MASW survey results were used to obtain the ground wave velocities including the longitudinal and shear wave velocity. The field velocities were used to calculate the small strain elastic moduli
f) Parameters that were interpreted in more two or more steps of the above were compared to each other
g) Finally, Correlations for both wet and natural conditions, using Gene Expression Programming, were conducted to obtain interrelations for deformability and strength in term of the measured parameters.

PLT was conducted according to ASTM-D1194 (1994)standard, using a plate of dimensions 700 mm × 700mm and three dial gauge as shown in Figure-1. The major steps in estimating the bearing capacity of soil using PLT results are as follows:

a) Plotting a stress (load divided by plate area) - average settlement curve.
b) Determined ultimate bearing capacity from the tangent intersection of the two straight portions of the stress - average settlement curve at the initial straight portion and the straight portion at the end.
c) Calculating allowable bearing capacity by dividing the ultimate bearing capacity by a factor of safety 2.5.

To calculate the modulus of subgrade reaction, the allowable settlement against allowable bearing capacity has been determined then the modulus of subgrade reaction calculate by dividing the allowable bearing capacity by the allowable settlement.

Some mechanical parameters like cohesion and angle of internal friction were estimated using the Terzagli equation and ultimate bearing capacity values obtained from PLT under the undrained (short term) and drained (long term) conditions. Under undrained conditions, the ultimate bearing capacity values were taken from the wet test then the value of cohesion is calculated. For the drained conditions case, the ultimate bearing capacity values were taken from the dry test then the angle of internal friction is determined by the trial and error method using two unknown variables, angle of internal friction and passive earth pressure coefficient.

UCS test was conducted according toASTM-D2938 (1995) standard. Figure-2 shows the typical setup of the UCS test.

SRT and MASW were conducted by implementing five seismic profiles 33 m long were carried out at five sites in Amman area (Adden, Dahyet Al-Yasameen, Marj Al-Hamam, ShafaBadran, and Abu Nusair). The seismic data was acquired using the 12-channel Smartseis seismograph™ and mechanical 10 kg

weight hammer used as the source of seismic energy. At each location, 13 mechanical source shots were performed, the first shot is 1.5 m away from the first geophone and the last shot is 1.5 m away from the last geophone. The spacing between the geophones is set to 3 m. Both of (P-waves and S-wave) were recorded using 4.5 Hz vertical geophones. The total record length was 1000 ms with sample interval of 0.5 ms.

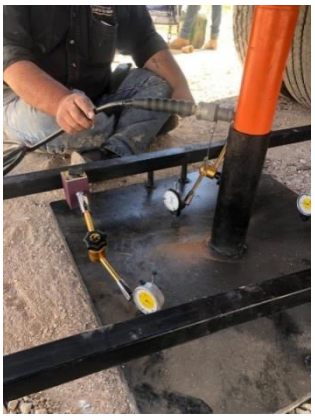


Figure-1. Plate Load Test Set Up Figure-2. Uniaxial Test Set Up.

Acquired SRT data were processed and interpreted using the software package SeisImager/2D (Pickwin & Plotrefa). The entire procedure for SRT consists of three stage:

a) Pickwin program was used to accurately pick the first breaks from the seismic signal for each shot record to obtain time-distance curves. The time-distance curves were constructed based on the geophone spacing, distance along the survey line, the first arrival time, and source location.
b) Using the Plotrefa program, time-distance curves created from each seismic line were analyzed. These curves were checked and corrected for the exact estimation of the P-waves velocity.
c) The velocity-depth profiles from recorded seismic velocity were modelled using a tomographic inversion method provided by the Plotrefa program. This method starts with an initial velocity model and iteratively traces rays through the model with the goal of minimizing the RMS (Root Mean Square)error between the observed and calculated travel times. The final depth-velocity models were then represented in 2D. This model converted the tomogram to a layered model to better represent the layered nature of the geology(Al-Saigh & Al-Heety, 2014).

The acquired MASW data processed and interpreted using SeisImager/SW software to determination of shear-wave velocity (Vs). The MASW procedure consists of three steps: obtaining multi-channel field records, processing the data to determine a dispersion curve, and inverting these dispersion curves to obtain 1-D (depth) Vs profiles(Park *et al.*, 2007).

The logical sequence of this study, in the beginning, conducted subsurface exploration, UCS test, PLT, SRT, and MASW. Then taken some data from the UCS test like density to calculate seismically moduli (Shear modulus, Young's modulus, and Bulk modulus). After that, the influence depth of footing at which we want to make a comparison was calculated.

Analysis and Results

The following sections represent the results of the field and lab testing along with the interpretations and quantitative analysis. The first section consists of drilling results and soil profiling, the second section is for the uniaxial compressive strength test, the plate load test, and finally the MASW survey.

Drilling and Coring

Ten boreholes were drilled at five sites in Ammanarea (Adden, Dahyet Al-Yasameen, Marj Al-Hamam, ShafaBadran, and Abu Nusair), in each site two boreholes were drilled and according to Table-1. Strater 5 software was used to develop the lithology and stratigraphy for the studied areas as shown in Figure-2.

ARPN Journal of Engineering and Applied Sciences

Table-1. Coordinates boreholes in the study area.

Site	BH	Latitude	Longitude	Depth (m)
Adden	BH-1	31.9437709	35.9759864	6
	BH-2	31.9436787	35.9761520	6
Dahyet Al-Yasameen	BH-1	31.9293622	35.8963214	6
	BH-2	31.9293015	35.8962296	6
Marj Al-Hamam	BH-1	31.8798509	35.8540609	6
	BH-2	31.8797220	35.8540864	6
ShafaBadran	BH-1	32.0324371	35.9076665	8
	BH-2	32.0324490	35.9078425	8
Abu Nusair	BH-1	32.0667252	35.8907830	8
	BH-2	32.0669085	35.8905165	8

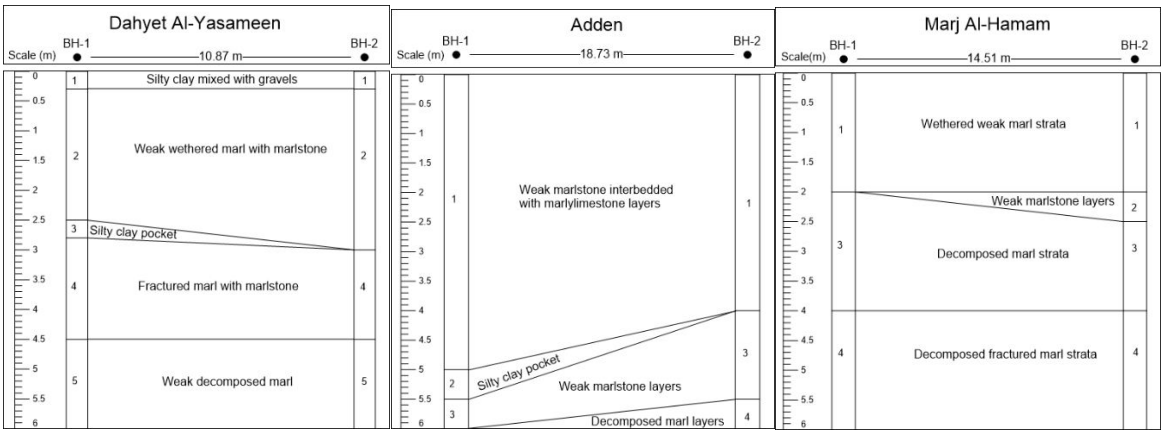

(a)Dahyet Al-Yasameen (b) Adden(c) Marj Al-Hamam

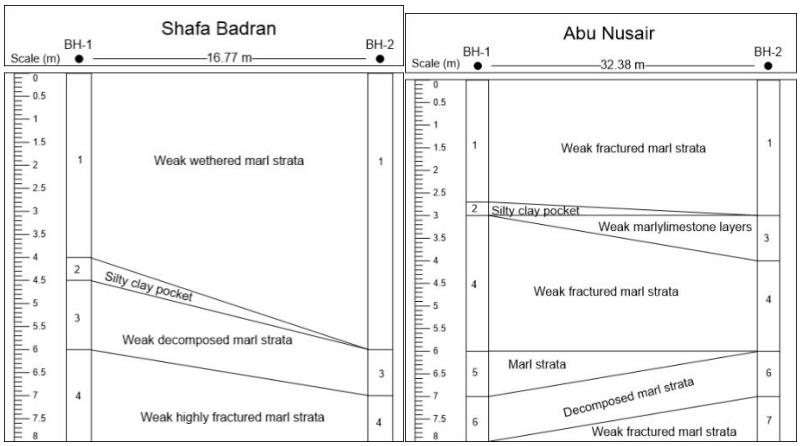

(d) Shafa Badran(e) Abu Nusair

Figure-2. Stratigraphic lithology for each site.

Unconfined Compression Strength (UCS) Test

The main purpose of this test was to determine the UCS of the Marl formations on the area. The maximum axial compressive stress that an intact rock core specimen can resist under unconfined conditions, i.e., when the confining stress is zero, is known as UCS (Alnuaim *et al*., 2019). During the drilling of geotechnical investigation boreholes, thirty specimens were collected from depths of 2 to 4 meters. Six specimens were taken from each site, three from each borehole, two dry specimens taken at a depth of 2 m and 4 m, and a wet specimen at a depth of 4 m. To perform UCS test, rock core specimens of 7.4 cm in diameter and 10 cm in length were taken from specimens. The results obtained from the UCS test for each site are presented in Figures (3 to 12). Accordingly, the compressive strength of each specimen

was determined. The most common approach to test rock elasticity and determine the elastic modulus (Young's modulus) is to use the stress-strain curve for axial deformations (Małkowski *et al.*, 2018). The Young's modulus of elasticity for rock material under uniaxial pressure can be calculated in three different ways: as a secant, as a tangent, and as an average modulus. The average Young's modulus method, which is defined as the slope of the straight-line part of the stress-strain curve for the given test, was used in this study. The average Young's modulus of each intact specimen was calculated using the following formula (Briševac *et al*., 2021; Małkowski *et al.,* 2018):

$$E_s = \frac{\Delta\sigma}{\Delta\varepsilon_a}$$

Where:
E_s: Average Young's modulus
$\Delta\sigma$: Change in axial stress from the initial linear segment of stress-strain curve
$\Delta\varepsilon_a$: Change in axial strain from the initial linear segment of stress-strain curve

Shear modulus can be determine, isotopically, using Poisson's ratio and the elastic modulus(Bowles, 1997):

$$\acute{G}_s = \frac{E_s}{2(1+\nu)}$$

Where:
$\acute{G}_s$: Shear modulus
v: Poisson's ratio.

On the basis of the seismic data, v was determined, and the value of v in the dry state was assumed to be equal to the value of μ in the wet state. The values of failure load, UCS,E_s, $\acute{G}_s$, and v for different rock core specimens are given in Table-2.

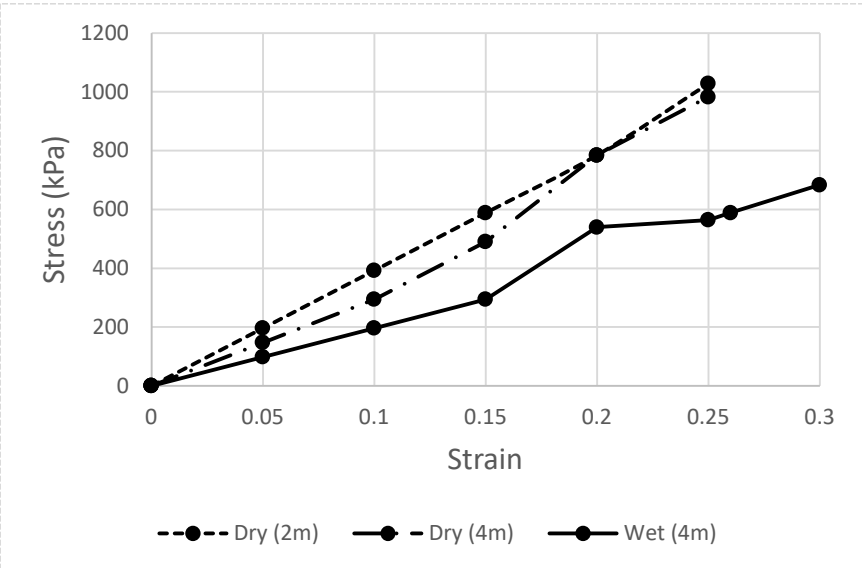

Figure-3. Stress - strain diagrams of Marj Al-Hamam (BH-1).

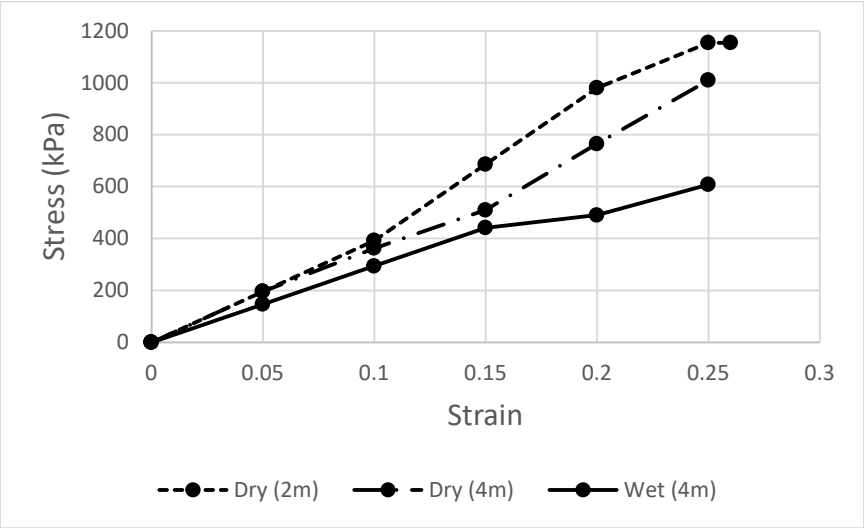

Figure-4. Stress - strain diagrams of Marj Al-Hamam (BH-2).

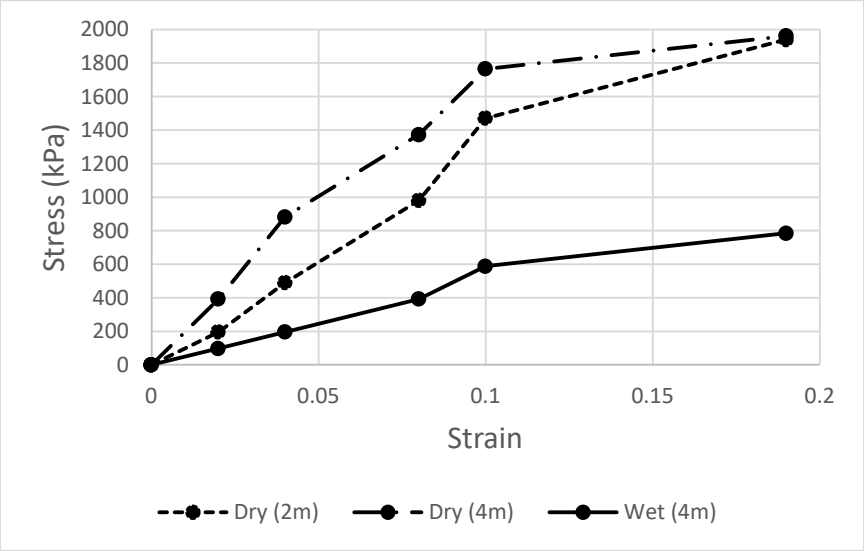

Figure-5. Stress - strain diagrams of Shafa Badran (BH-1).

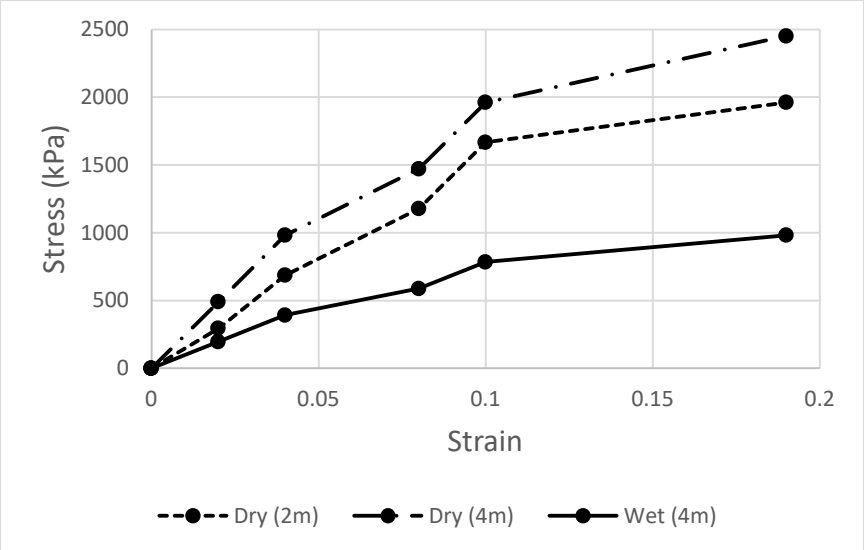

Figure-6. Stress - strain diagrams of Shafa Badran (BH-2).

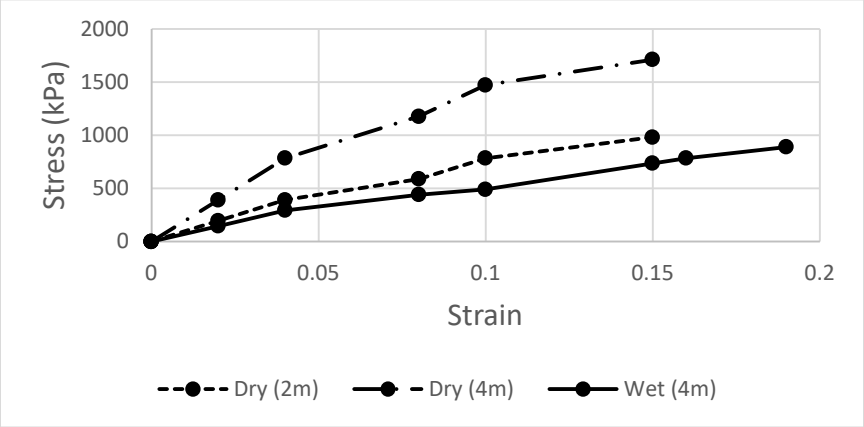

Figure-7. Stress - strain diagrams of Abu Nusair (BH-1).

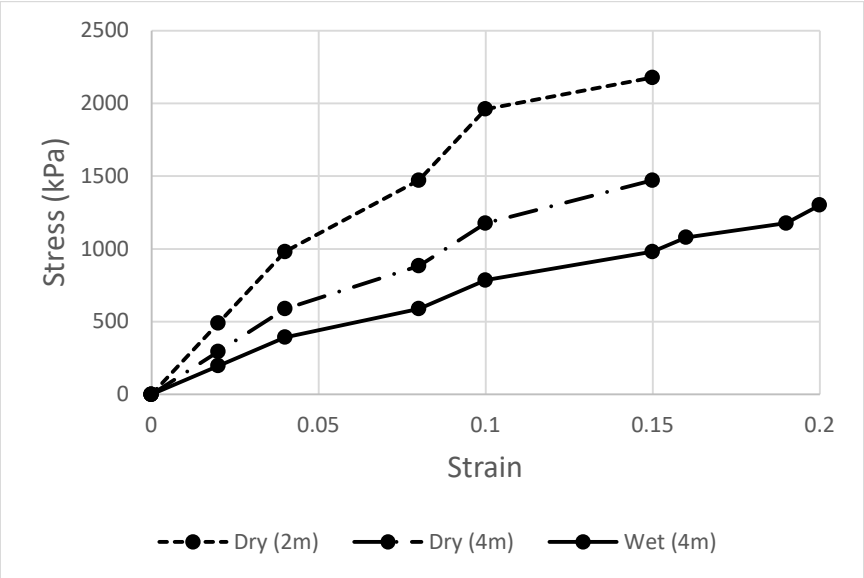

Figure-8. Stress - strain diagrams of Abu Nusair (BH-2).

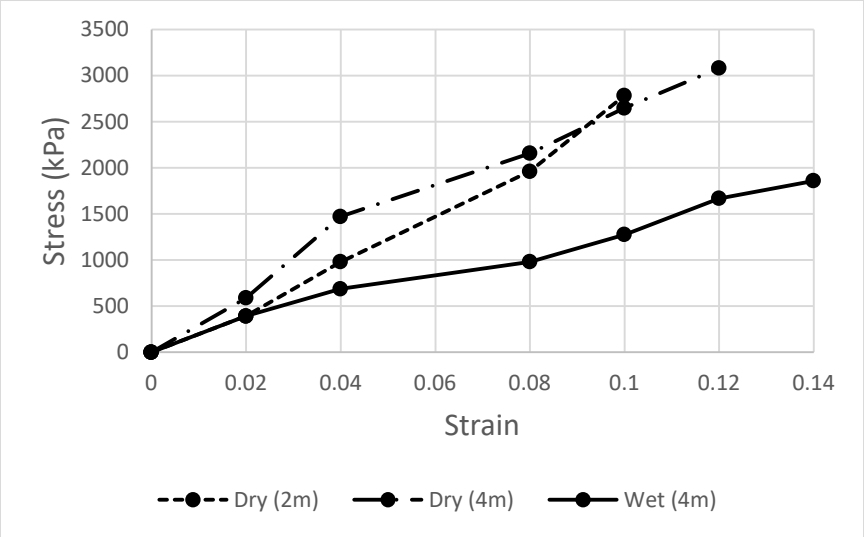

Figure-9. Stress - strain diagrams of Adden (BH-1).

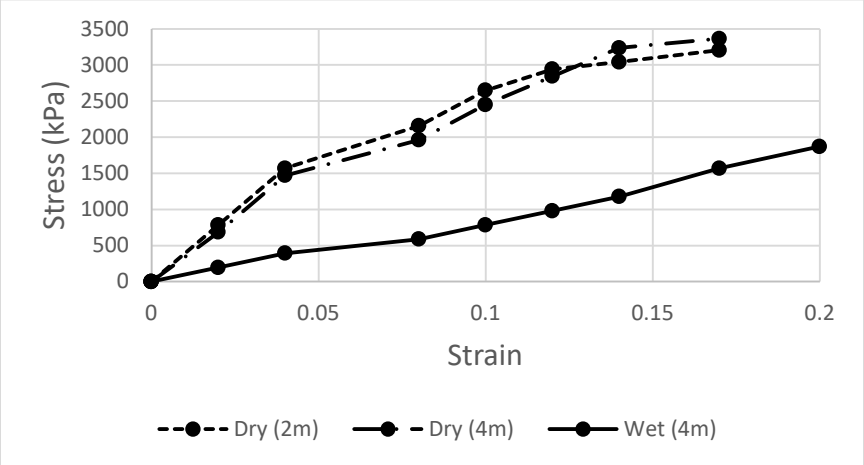

Figure-10. Stress - strain diagrams of Adden (BH-2).

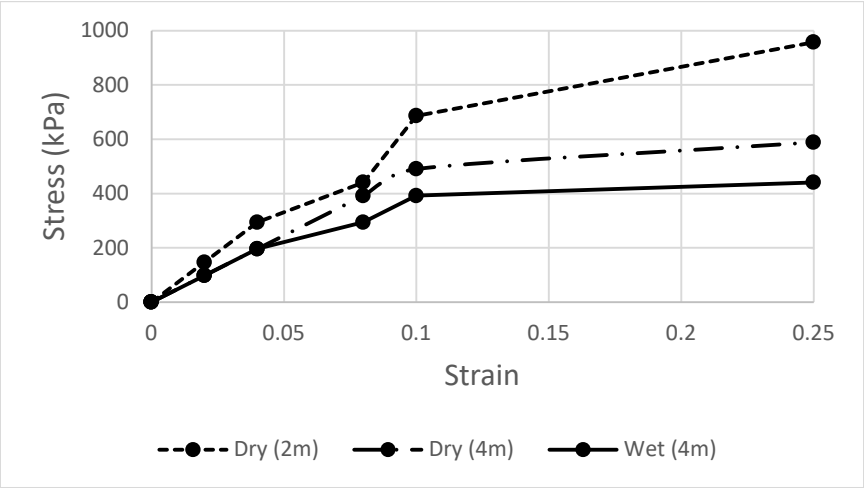

Figure-11. Stress - strain diagrams of Dahyet Al-Yasameen (BH-1).

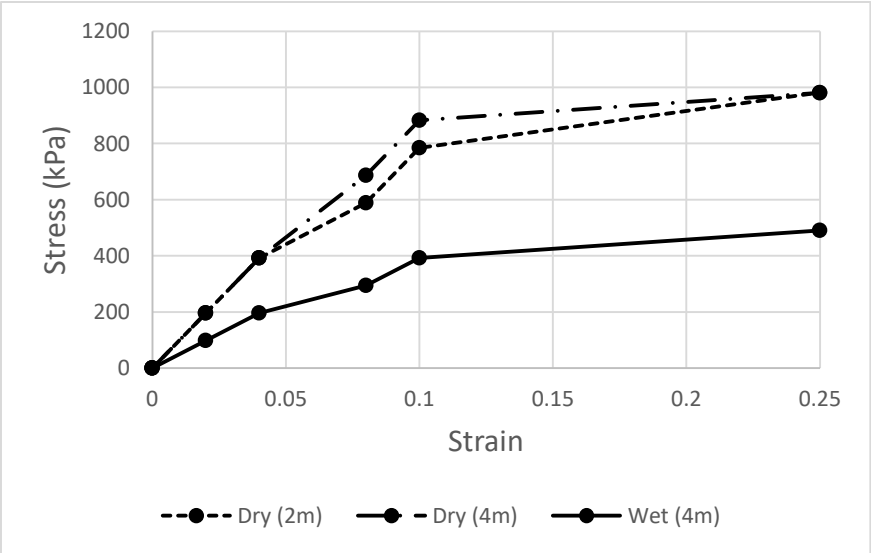

Figure-12. Stress - strain diagrams of Dahyet Al-Yasameen (BH-2).

Table-2. Characteristics of rock core specimens.

Site	BH	Depth (m)	Failure load (kN)	UCS (kPa)	v	E_s (kPa)	$\acute{G}_s$ (kPa)
Marj Al-Hamam	BH-1 Dry	2	2.53	588.42	0.24	3985.56	1607.08
	BH-1 Dry	4	2.11	490.35	0.24	2942.10	1186.33
	BH-1 Wet	4	1.26	294.21	0.24	1961.40	790.89
	BH-2 Dry	2	2.95	686.49	0.24	3922.80	1581.77
	BH-2 Dry	4	2.19	509.96	0.24	3726.66	1502.69
	BH-2 Wet	4	1.90	441.32	0.24	2942.10	1186.33
ShafaBadran	BH-1 Dry	2	6.32	1471.05	0.30	9807.00	3771.92
	BH-1 Dry	4	7.59	1765.26	0.39	21248.50	7643.35
	BH-1 Wet	4	2.53	588.42	0.39	4903.50	1763.85
	BH-2 Dry	2	7.17	1667.19	0.30	16345.00	6286.54
	BH-2 Dry	4	8.43	1961.40	0.39	24517.50	8819.24
	BH-2 Wet	4	3.37	784.56	0.39	9807.00	3527.70
Abu Nusair	BH-1 Dry	2	3.37	784.56	0.33	9807.00	3686.84
	BH-1 Dry	4	6.32	1471.05	0.25	19614.00	13076.00
	BH-1 Wet	4	2.11	490.35	0.25	7355.25	4903.50
	BH-2 Dry	2	8.43	1961.40	0.33	24517.50	9217.11
	BH-2 Dry	4	5.06	1176.84	0.25	14710.50	9807.00
	BH-2 Wet	4	3.37	784.56	0.25	9807.00	6538.00
Adden	BH-1 Dry	2	11.55	2687.85	0.16	19614.00	8454.31
	BH-1 Dry	4	12.91	3001.01	0.23	29421.00	11959.76
	BH-1 Wet	4	5.58	1299.37	0.23	19614.00	7973.17
	BH-2 Dry	2	13.30	3095.10	0.16	39228.00	16908.62
	BH-2 Dry	4	14.10	3279.13	0.23	35959.00	14617.48
	BH-2 Wet	4	5.62	1307.60	0.23	9807.00	3986.59
Dahyet Al-Yasameen	BH-1 Dry	2	3.34	776.71	0.14	7355.25	4276.31
	BH-1 Dry	4	2.11	490.35	0.24	4903.50	1977.22
	BH-1 Wet	4	1.69	392.28	0.24	4903.50	1977.22
	BH-2 Dry	2	3.65	850.27	0.14	9807.00	5701.74
	BH-2 Dry	4	3.93	915.32	0.24	9807.00	3954.44
	BH-2 Wet	4	1.83	424.97	0.24	4903.50	1977.22

Table-3 shows density measurements obtained from boreholes samples at several depths while Table 4 shows mechanical and hydraulic parameters at each site.

Plate Loading Tests (PLT)

Fourteen PLT were carried out at five sites in Amman area (Adden, Dahyet Al-Yasameen, Marj Al-Hamam, ShafaBadran, and Abu Nusair). Two tests were performed for each site, one in the dry condition and the other in the wet condition. The test was conducted twice in Dahyet Al-Yasameen and Marj Al-Hamam. Figures (13 to 19) include the results of the PLT for each site, so that was drawn of stress versus average settlement.

Table-3. Density measurements.

Site	BH	Depth (m)	Density (kg/m^3)
Shafa Badran	BH-1	2	1650
	BH-1	4	1750
	BH-2	2	1750
	BH-2	4	1850
Abu Nusair	BH-1	2	1660
	BH-1	4	1800
	BH-2	2	1870
	BH-2	4	1720
Dahyet Al-Yasameen	BH-1	2	1980
	BH-1	4	1950
	BH-2	2	1990
	BH-2	4	1980
Marj Al-Hamam	BH-1	2	1530
	BH-1	4	1610
	BH-2	2	1590
	BH-2	4	1650
Adden	BH-1	2	1907
	BH-1	4	2103
	BH-2	2	2232
	BH-2	4	2242

Table-4. Mechanical and hydraulic parameters.

Site	BH	Specific gravity	Cohesion (c) (kPa)	Friction angle (ϕ)	Permeability (mm/s)	Moisture content (%)
Adden	BH-1	2.15	76.4946	30	0.03541	3
	BH-2	2.19	85.3209	30	.....	3
Dahyet Al-Yasameen	BH-1	2.107	47.0736	18	.....	10
	BH-2	2.095	49.0350	18	0.7050	10
ShafaBadran	BH-1	2.01	87.2823	20	.....	5
	BH-2	2.20	113.7612	20	0.6530	4
Marj Al-Hamam	BH-1	2.07	49.0350	18	0.8427	6
	BH-2	2.088	55.8999	18	.....	6
Abu Nusair	BH-1	2.09	53.9385	18	.....	7
	BH-2	2.01	97.0893	18	0.04672	7

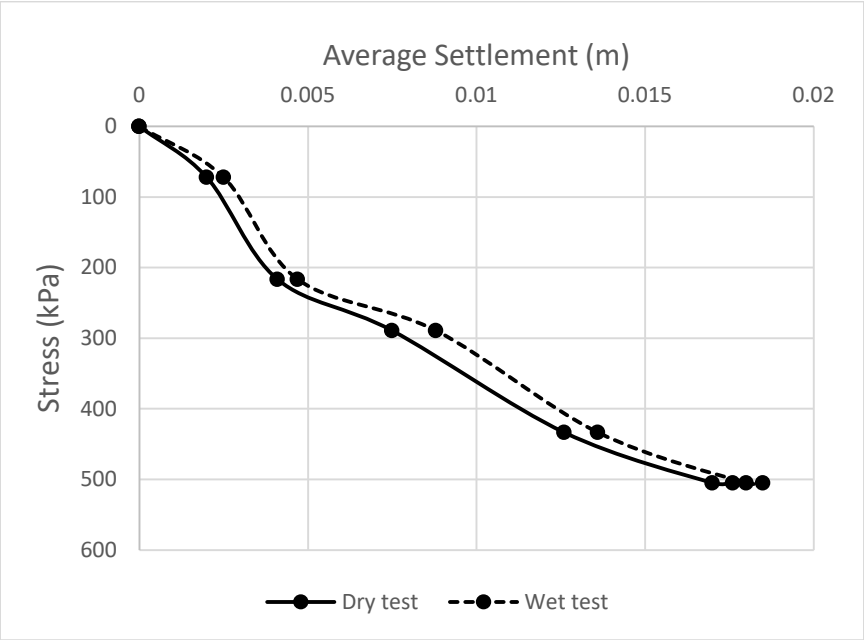

Figure-13. Stress -average settlement diagrams of Adden.

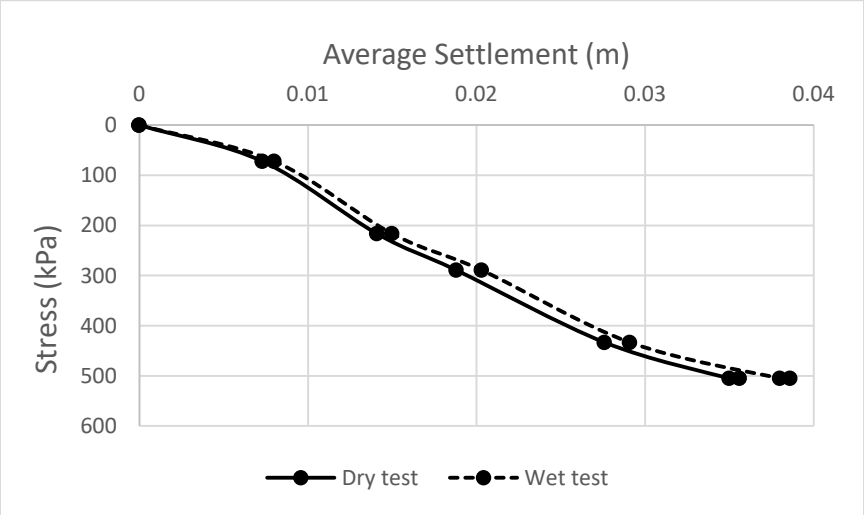

Figure-14. Stress - average settlement diagrams of Dahyet Al-Yasameen (1).

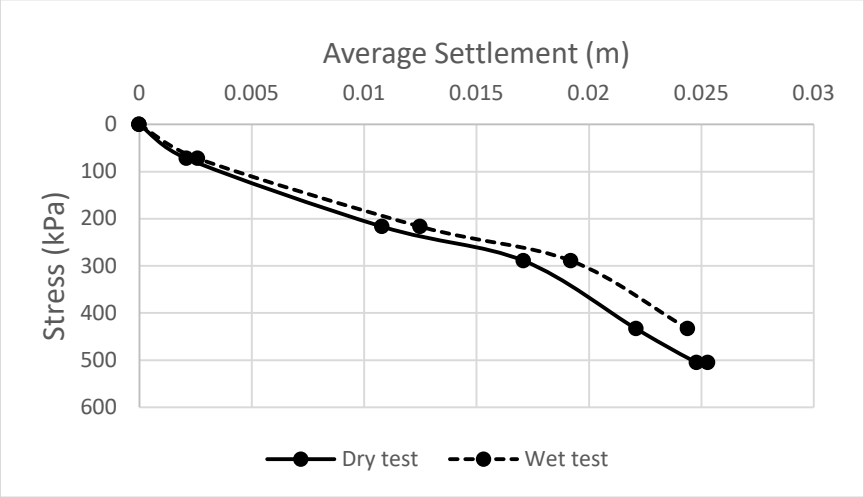

Figure-15. Stress - average settlement diagrams of Marj Al-Hamam (1).

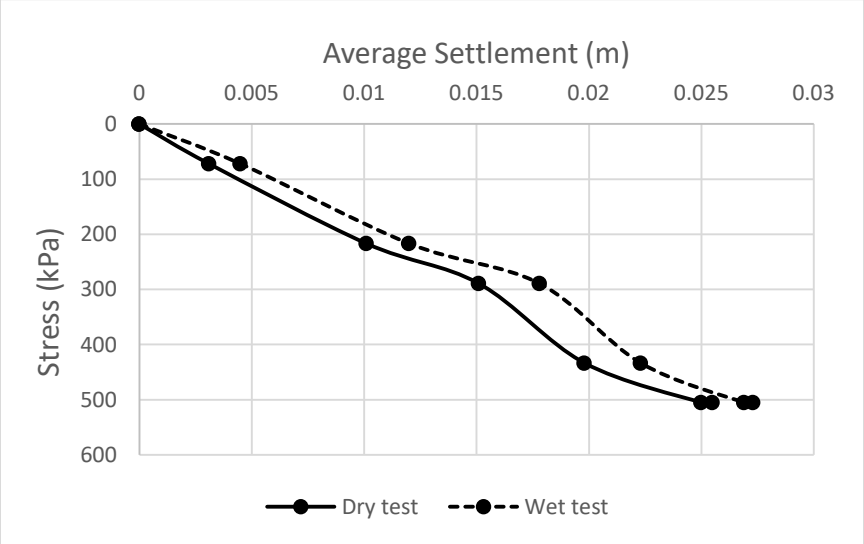

Figure-16. Stress - average settlement diagrams of Abu Nusair.

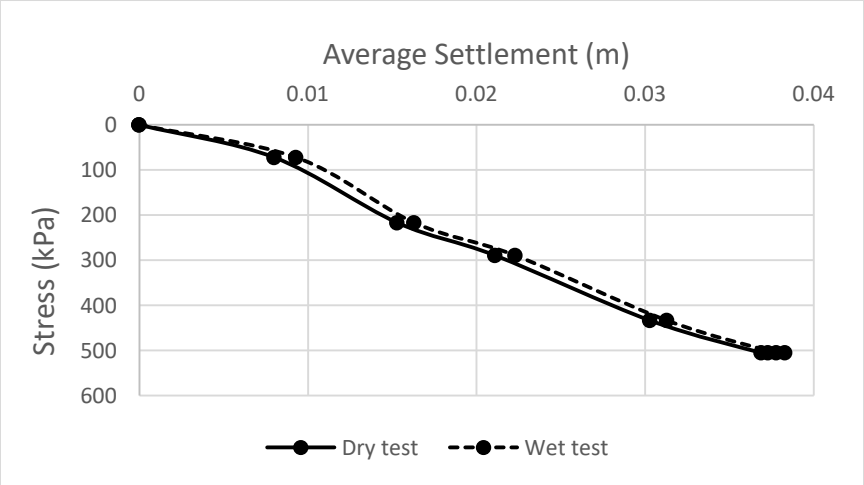

Figure-17. Stress - average settlement diagrams of Shafa Badran.

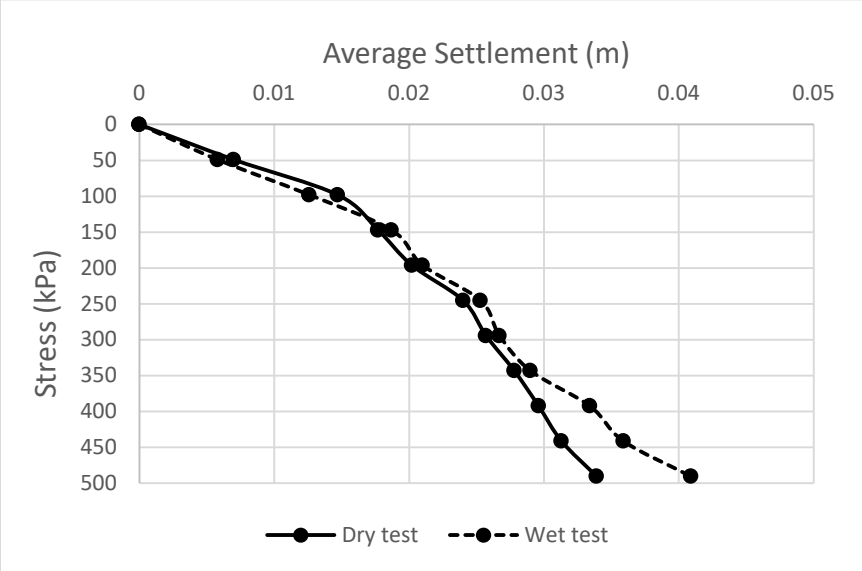

Figure-18. Stress - average settlement diagrams of Dahyet Al-Yasameen (2).

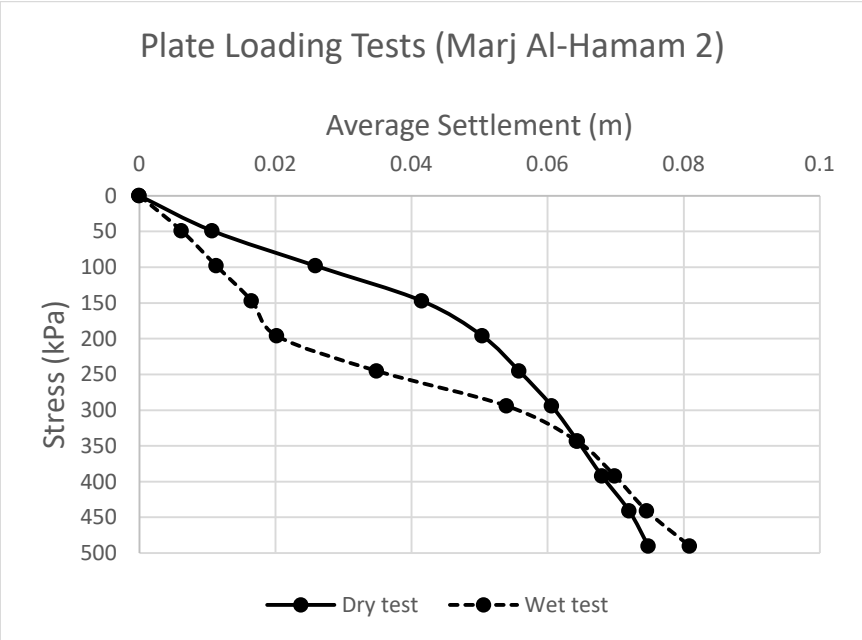

Figure-19. Stress - average settlement diagrams of Marj Al-Hamam (2).

Plate load test, in principle, was used in this study to estimate the ultimate bearing capacity, modulus of subgrade. Based on these parameters, elastic moduli and the shear strength parameters were determined according back analysis procedures. Plate load test procedures can be summarized as follows:

a) The ultimate bearing capacity has been determined from the tangent intersection of the two straight portions of the stress - average settlement curve at the initial straight portion and the straight portion at the end (Adams & Collin, 1997).

b) The allowable bearing capacity was calculated as(Bowles, 1997):

$$q_{all} = \frac{q_{ult}}{SF}$$

Whereq_{all} is the allowable bearing capacity (KPa), $q_{ult}$is the ultimate bearing capacity (KPa), and $SF$is a safety factor usually taken as 2.5 in this study.

c) The coefficient of subgrade reaction k_s was calculated as (Lin *et al.*, 1998):

$$k_s = \frac{q_{all}}{\delta_{all}}$$

Where k_s is the modulus of subgrade reaction (kN/m^3), and δ_{all} is the allowable settlement against q= q_{all}, meter. The values of q_{ult},q_{all} ,δ_{all}, and $K_s$are given in Table-5.

Table-5. q_{ult},q_{all} ,δ_{all}, and K_s values.

Site	Test	q_{ult} (kPa)	q_{all} (kPa)	δ_{all}(m)	K_s (kN/m^3)
Adden	Dry	280.00	112.00	0.0026	43444.53
	Wet	280.00	112.00	0.0031	36059.24
Dahyet Al-Yasameen (1)	Dry	360.00	144.00	0.0107	13485.67
	Wet	360.00	144.00	0.0115	12545.74
Marj Al-Hamam (1)	Dry	289.31	115.72	0.0047	24512.31
	Wet	289.31	115.72	0.0056	20731.39
Abu Nusair	Dry	289.31	115.72	0.0052	22215.90
	Wet	289.31	115.72	0.0068	17121.26
ShafaBadran	Dry	289.31	115.72	0.0102	11346.47
	Wet	289.31	115.72	0.0114	10143.10
Dahyet Al-Yasameen (2)	Dry	130.00	52.00	0.0075	6964.91
	Wet	190.00	76.00	0.0095	7967.29
Marj Al-Hamam (2)	Dry	180.00	72.00	0.0178	4040.63
	Wet	294.21	117.68	0.0134	8795.52

Using the elastic parameters (E_s, μ), the modulus of subgrade reaction was also determined using the formula proposed by Meyerhof and Baike(Avci & Gurbuz, 2018).

$$K_s = \frac{E_s}{B(1-\mu^2)}$$

Where B is the width of footing.μ was determined from seismic data and was taken from the nearest surface layer.

Table-6 shows the calculation of $K_s$using E_s from the UCS test while Table-7 shows the calculation of $K_s$usingE_s from the seismic data.

Table-6. $K_s$calculated values using $E_s$from the UCS test.

Site	BH	Depth (m)	v	E_s (kPa)	B (m)	K_s (kN/m^3)
ShafaBadran	BH-1	2	0.30	9807.00	0.7	15395.60
	BH-2	2	0.30	16345.00	0.7	25659.34
Abu Nusair	BH-1	2	0.33	9807.00	0.7	15722.14
	BH-2	2	0.33	24517.50	0.7	39305.35
Dahyet Al-Yasameen	BH-1	2	0.14	7355.25	0.7	10717.56
	BH-2	2	0.14	9807.00	0.7	14290.09
Marj Al-Hamam	BH-1	2	0.24	3985.56	0.7	6041.66
	BH-2	2	0.24	3922.80	0.7	5946.52
Adden	BH-1	2	0.16	19614.00	0.7	28756.16
	BH-2	2	0.16	39228.00	0.7	57512.32

Table-7. K_s calculated values using E_s from the seismic data.

Site	μ	E_s (kPa)	B (m)	K_s (kN/m3)
ShafaBadran.	0.30	622895.00	0.7	977857.14
Abu Nusair	0.33	949370.63	0.7	1521988.27
Dahyet Al-Yasameen	0.14	2751570.00	0.7	4009398.50
Marj Al-Hamam	0.24	1775668.84	0.7	2691712.41
Adden	0.16	4347948.19	0.7	6374542.86

Using the same equation, E_s was calculated using $K_s$calculated from the PLT. Then E_s was used to calculate $\acute{G}_s$ as shown in Table-8.

Table-8. E_s and $\acute{G}_s$calculatedvalues.

Site	Test	K_s(kN/m^3)	v	$B(m)$	E_s(kPa)	$\acute{G}_s$ (kPa)
Adden	Dry	43444.53	0.16	0.7	29632.65	12772.69
	Wet	36059.24	0.16	0.7	24595.29	10601.42
Dahyet Al-Yasameen (1)	Dry	13485.67	0.14	0.7	9254.95	5380.78
	Wet	12545.74	0.14	0.7	8609.89	5005.75
Marj Al-Hamam (1)	Dry	24512.31	0.24	0.7	16170.28	6520.27
	Wet	20731.39	0.24	0.7	13676.08	5514.55
Abu Nusair	Dry	22215.90	0.33	0.7	13857.61	5209.63
	Wet	17121.26	0.33	0.7	10679.73	4014.94
ShafaBadran	Dry	11346.47	0.30	0.7	7227.70	2779.88
	Wet	10143.10	0.30	0.7	6461.15	2485.06
Dahyet Al-Yasameen (2)	Dry	6964.91	0.14	0.7	4779.88	2779.00
	Wet	7967.29	0.14	0.7	5467.79	3178.95
Marj Al-Hamam (2)	Dry	4040.63	0.24	0.7	2665.52	1074.81
	Wet	8795.52	0.24	0.7	5802.23	2339.61

According to Terzagli bearing capacity theory, the bearing capacity of the general shear failure mode for a square footing can be calculated using the following equation(Bowles, 1997):

$$q_{ult} = 1.3cN_c + \bar{q}N_q + 0.4\gamma_2 BN_\gamma$$

Where:

c:	cohesion
$\bar{q}$:	overburden pressure at the base of the foundation $=\gamma_1 D$
D:	footing depth (at the bottom)
γ_1:	unit weight of soil above foundation level
γ_2:	unit weight of soil below foundation level
B:	width of footing
N_c , N_q, N_γ:	bearing capacity factors depend on the angle of internal friction ϕ

Using the Terzagli equation and q_{ult}values obtained from PLT, the c and ϕ were estimated under the undrained (short term) and drained (long term) conditions. Because the footing was located on the ground surface, the $\bar{q}$=0.

In undrained conditions (ϕ = 0), the last part of the equation is zero, therefore the equation becomes as follows$q_{ult} = 1.3cN_c$,$q_{ult}$was taken from the wet test then the c was calculated.

The first part of the equation was assumed to be zero in drained conditions, therefore the equation becomes as follows $q_{ult} = 0.4\gamma BN_\gamma$, q_{ult} was taken from the dry test then the ϕ was determined by the trial and error method using two unknown variables, ϕ and passive earth pressure coefficient($K_{p\gamma}$). So that the ϕ and the value of the associated $K_{p\gamma}$are compensated until both sides of the equation are equal.

Moreover, the influence depth of footing was calculated according to the following equation (Bowles, 1997):

$$H = \frac{B}{2}\tan(\alpha)$$

Where H is the influence depth of footing, and α is the angle.Terzagli used (α = ϕ). The values of c, ϕ,$K_{p\gamma}$, γ, and H are given in Table-9.

Table-9. c, ϕ,$K_{p\gamma}$,γ and H values.

Site	Drained conditions	Undrained conditions	$K_{p\gamma}$	γ (kN/m^3)	H (m)
	c (kPa)	ϕ (deg.)			
Adden	37.79	35.747	90.8146	20.301795	0.2519
Dahyet Al-Yasameen (1)	48.58	37.364	109.8952	19.47285	0.2672
Marj Al-Hamam (1)	39.04	37.494	111.4292	15.3036	0.2685
Abu Nusair	39.04	36.783	103.0394	17.31465	0.2617
ShafaBadran	39.04	36.996	105.5528	16.677	0.2637
Dahyet Al-Yasameen (2)	25.64	31.11	58.66	19.47285	0.2112
Marj Al-Hamam (2)	39.70	34.93	81.58	15.3036	0.2444

Seismic Refraction Tomography (SRT) and Multi-Channel Analysis of Surface Waves (MASW)

The interpretations of five seismic profiles for P-wave models and S-wave models were plotted for the five sites as shown in Figures (20 to24).

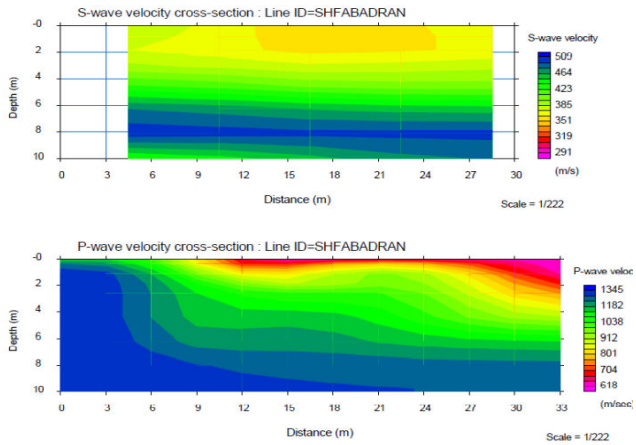

Figure-20. Geoseismic model interpretation at ShafaBadran.

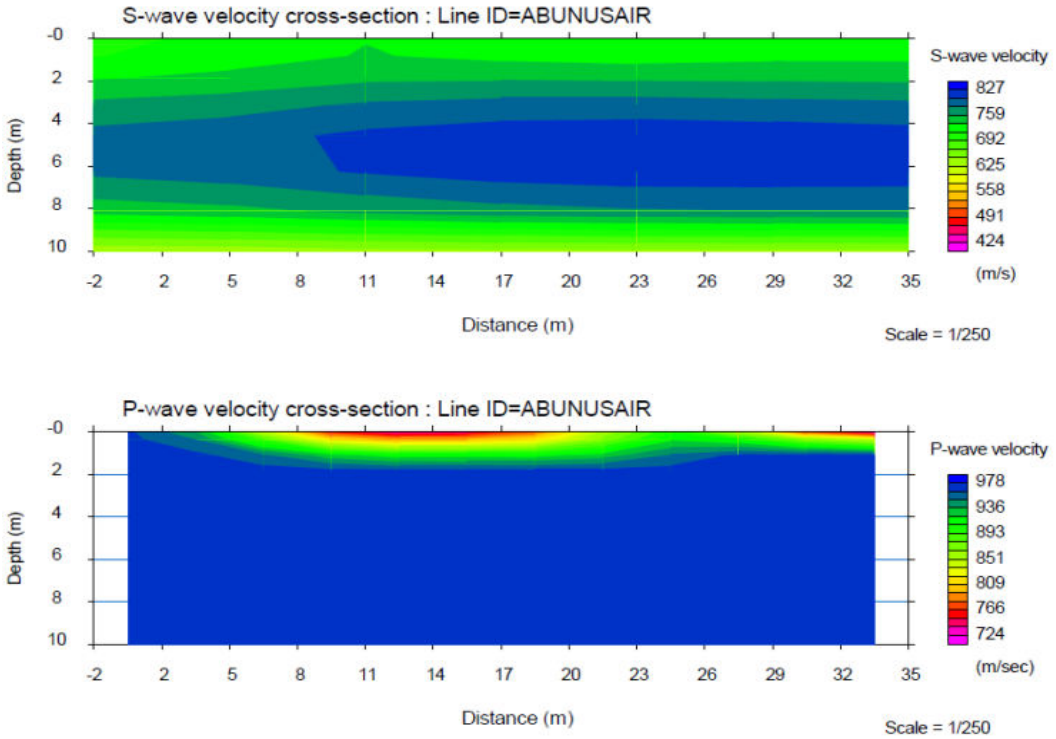

Figure-21. Geoseismic model interpretation at Abu Nusair.

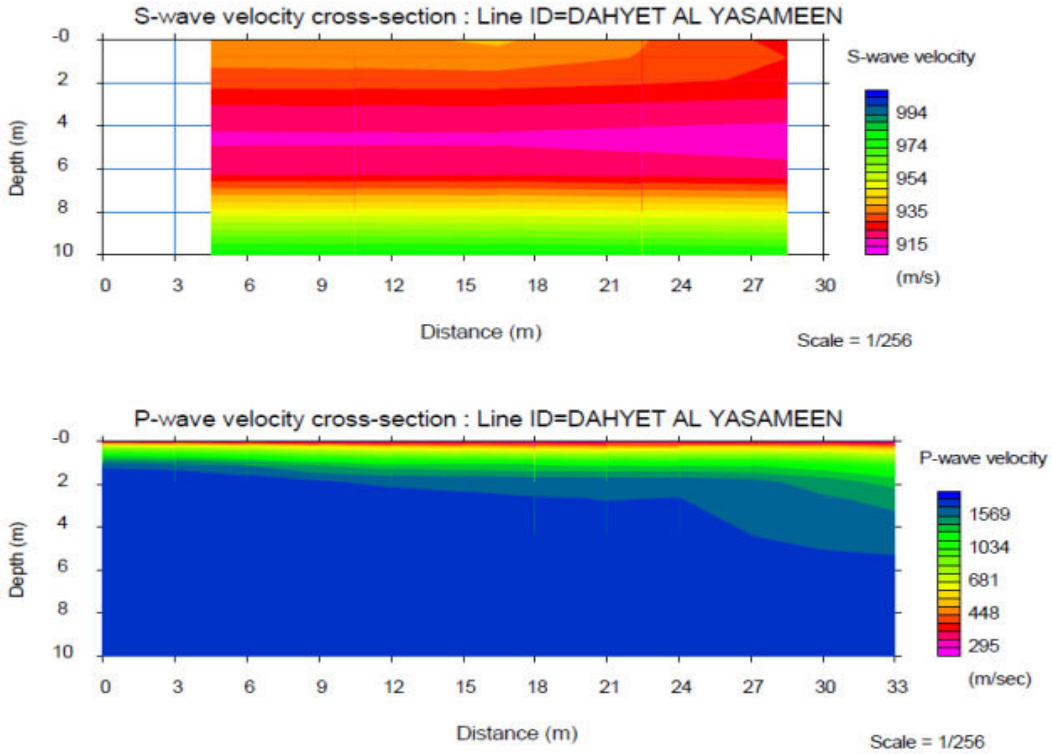

Figure-22. Geoseismic model interpretation at Dahyet Al-Yasameen.

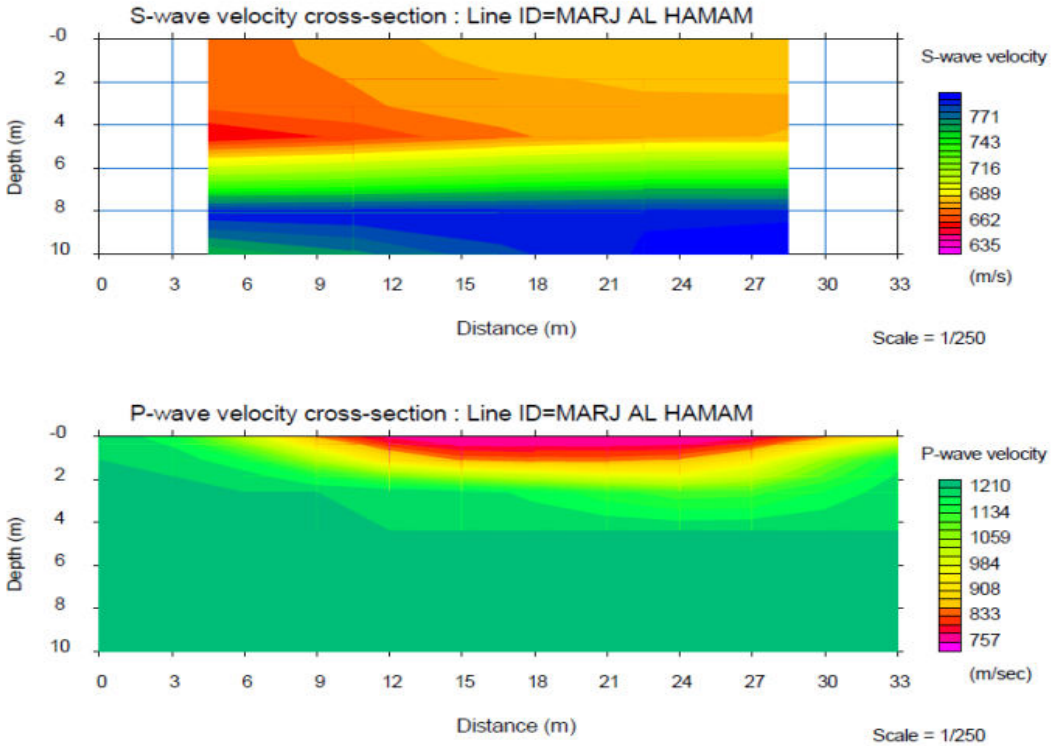

Figure-23. Geoseismic model interpretation at Marj Al-Hamam.

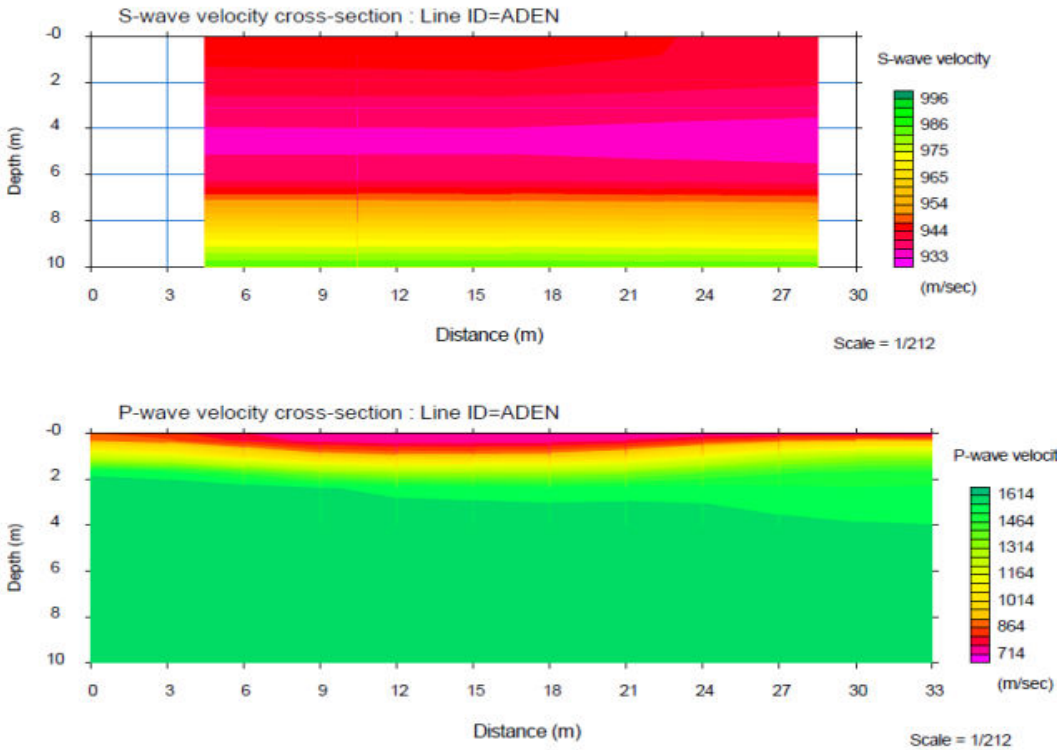

Figure-24. Geoseismic model interpretation at Adden.

For a better engineering understanding of the subsurface layers, the elastic moduli can be estimated using seismic velocities (Vp and Vs) obtained by MASW and SRT methods (Khalil & Hanafy, 2016). To calculate elastic moduli (E_s, $\acute{G}_s$, v and Bulk modulus (K)) we are using the equations are given in Table-10 based on the average density (ρ) measurements obtained from boreholes samples. Table-11 shows the input forward parameters (Vp, Vs, and ρ) used to calculate geotechnical elastic moduli.

Table-12 summarizes the $\acute{G}_s$and $E_s$calculated from the UCS test and from the seismic data for all sites as mentioned in Tables 2 and 11 in addition to the relation between them in the approximate depth. The $\acute{G}_s$ and $E_s$were calculated from the UCS test according to the two equations mentioned earlier after drawing a stress-strain diagram. On the basis of the seismic data. μ was determined, the value of μ in the dry state was assumed to be equal to the value of μ in the wet state. The $\acute{G}_s$and $E_s$were calculated from the seismic data according to the equations mentioned earlier in Table-10. After that made the relation between E_s calculated from seismic data and E_s calculated from the UCS test in the approximate depth also was made the relation between $\acute{G}_s$calculated from seismic data and $\acute{G}_s$ calculated from the UCS test in the approximate depth

Table-10. Elastic moduli equations.

Elastic moduli	Used formula	Reference
Poisson's Ratio (μ)	$\mu = \frac{{V_P}^2 - 2{V_S}^2}{2({V_P}^2 - {V_S}^2)}$	(Diene & Ndiaye, 2022)
Shear Modulus ($\acute{G}_s$)	$\acute{G}_s = \rho {V_S}^2$	(Birch, 1961)
Young's Modulus (E_s)	$E_s = 2\rho {V_S}^2(1+\mu)$	(Park, 2013)
Bulk modulus (K)	$K = \rho\left({V_P}^2 - \left(\frac{4}{3}\right){V_S}^2\right)$	(Birch, 1961)

Table-11. Geotechnical data calculations based on seismic survey at five seismic sites.

Borehole	From (m)	To (m)	Thickness h (m)	Vp m/s	Vs m/s	ρ (kg/m^3)	v	Lithology	K (N/m^2)	$\acute{G}_s$ (N/m^2)	E_s (N/m^2)
Shafa Badran	**0**	**3**	**3**	**689**	**370**	1750.0	**0.30**	**Top soil**	**5.11×10^8**	**2.40×10^8**	**6.23×10^8**
	3	6	3	1050	450		0.39	Yellow weak Marlstone layers	1.46×10^9	3.54×10^8	9.85×10^8
	6	10	4	1355	515		0.42	Yellow weak wet Marl strata	2.59×10^9	4.64×10^8	1.32×10^9
Abu Nusair	0	2	2	900	450	1762.5	0.33	Top soil	9.52×10^8	3.57×10^8	9.49×10^8
	2	6	4	980	760		0.25	Yellow weak fractured Marlstone layers	3.35×10^8	1.02×10^9	1.53×10^9
	6	10	4	980	600		0.20	Yellow weak Marl strata	8.47×10^8	6.35×10^8	1.52×10^9
Dahyet Al-Yasameen	0	2	2	1200	900	1975.0	0.14	Top soil	7.11×10^8	1.60×10^9	2.75×10^9
	2	7	5	1600	940		0.24	Yellow weak fractured Marl layers	2.73×10^9	1.75×10^9	4.33×10^9
	7	10	3	1600	990		0.19	Yellow weak fractured Marl layers	2.48×10^9	1.94×10^9	4.61×10^9
Marj Al-Hamam	0	4	4	1150	670	1595.0	0.24	Yellow weak fractured Marlstone layers	1.15×10^9	7.16×10^8	1.78×10^9
	4	10	6	1250	760		0.21	Yellow weak Marl strata	1.26×10^9	9.21×10^8	2.23×10^9
Adden	0	2	2	1480	940	2121.0	0.16	Yellow to white weak Marlstone layers	2.15×10^9	1.87×10^9	4.35×10^9
	2	10	8	1650	980		0.23	Yellow to white weak Marlstone layers	3.06×10^9	2.04×10^9	5.01×10^9

Table-12. Seismic modulus and unconfined compression strength modulus in addition to the relation between them.

Seismic Modulus						Unconfined Compression Strength Modulus						
Site name	**From (m)**	**To (m)**	***v***	**$\acute{G}_s$ (N/m^2)**	**E_s (N/m^2)**	**BH**	**Depth (m)**	Type ed ***v***	**E_s (N/m^2)**	**$\acute{G}_s$ (N/m^2)**	**$E_s$seis/E_s uncon**	**$\acute{G}_s$seis /$\acute{G}_s$uncon**
Shafa Badran.	0	3	0.30	$2.40*10^8$	$6.23*10^8$	BH-1 Dry	2	0.30	$9.81*10^6$	$3.77*10^6$	63.52	63.52
						BH-1 Dry	4	0.39	$2.12*10^7$	$7.64*10^6$	46.36	46.36
	3	6	0.39	$3.54*10^8$	$9.85*10^8$	BH-1 Wet	4	0.39	$4.9*10^6$	$1.76*10^6$	200.91	200.91
						BH-2 Dry	2	0.30	$1.63*10^7$	$6.29*10^6$	38.11	38.11
	6	10	0.42	$4.64*10^8$	$1.32*10^9$	BH-2 Dry	4	0.39	$2.45*10^7$	$8.82*10^6$	40.18	40.18
						BH-2 Wet	4	0.39	$9.81*10^6$	$3.53*10^6$	100.46	100.46
Abu Nusair	0	2	0.33	$3.57*10^8$	$9.49*10^8$	BH-1 Dry	2	0.33	$9.81*10^6$	$3.69*10^6$	96.81	96.81
						BH-1 Dry	4	0.25	$1.96*10^7$	$1.31*10^7$	77.85	77.85
	2	6	0.25	$1.02*10^9$	$1.53*10^9$	BH-1 Wet	4	0.25	$7.36*10^6$	$4.90*10^6$	207.61	207.61
						BH-2 Dry	2	0.33	$2.45*10^7$	$9.22*10^6$	38.72	38.72
	6	10	0.20	$6.35*10^8$	$1.52*10^9$	BH-2 Dry	4	0.25	$1.47*10^7$	$9.81*10^6$	103.81	103.81
						BH-2 Wet	4	0.25	$9.81*10^6$	$6.54*10^6$	155.71	155.71
Dahyet Al-Yasameen	0	2	0.14	$1.60*10^9$	$2.75*10^9$	BH-1 Dry	2	0.14	$7.36*10^6$	$4.28*10^6$	374.10	374.10
						BH-1 Dry	4	0.24	$4.90*10^6$	$1.98*10^6$	882.61	882.61
	2	7	0.24	$1.75*10^9$	$4.33*10^9$	BH-1 Wet	4	0.24	$4.90*10^6$	$1.98*10^6$	882.61	882.61
						BH-2 Dry	2	0.14	$9.81*10^6$	$5.70*10^6$	280.57	280.57
	7	10	0.19	$1.94*10^9$	$4.61*10^9$	BH-2 Dry	4	0.24	$9.81*10^6$	$3.95*10^6$	441.30	441.30
						BH-2 Wet	4	0.24	$4.90*10^6$	$1.98*10^6$	882.61	882.61
Marj Al-Hamam	0	4	0.24	$7.16*10^8$	$1.78*10^9$	BH-1 Dry	2	0.24	$3.99*10^6$	$1.61*10^6$	445.53	445.53
						BH-1 Dry	4	0.24	$2.94*10^6$	$1.19*10^6$	603.54	603.54
						BH-1 Wet	4	0.24	$1.96*10^6$	$7.91*10^5$	905.31	905.31
	4	10	0.21	$9.21*10^8$	$2.23*10^9$	BH-2 Dry	2	0.24	$3.92*10^6$	$1.58*10^6$	452.65	452.65
						BH-2 Dry	4	0.24	$3.73*10^6$	$1.50*10^6$	476.48	476.48
						BH-2 Wet	4	0.24	$2.94*10^6$	$1.19*10^6$	603.54	603.54
Adden	0	2	0.16	$1.87*10^9$	$4.35*10^9$	BH-1 Dry	2	0.16	$1.96*10^7$	$8.45*10^6$	221.68	221.68
						BH-1 Dry	4	0.23	$2.94*10^7$	$1.20*10^7$	170.32	170.32
						BH-1 Wet	4	0.23	$1.96*10^7$	$7.97*10^6$	255.48	255.48
	2	10	0.23	$2.04*10^9$	$5.01*10^9$	BH-2 Dry	2	0.16	$3.92*10^7$	$1.69*10^7$	110.84	110.84
						BH-2 Dry	4	0.23	$3.60*10^7$	$1.46*10^7$	139.35	139.35
						BH-2 Wet	4	0.23	$9.81*10^6$	$3.99*10^6$	510.97	510.97

CONCLUSIONS

The shear strength and deformability parameters were successfully studied according to the unconfined compressive strength (UCS), the plate Load Test (PLT), the Multi-Channel Analysis of Seismic Waves (MASW), and the rock index properties. The elastic soil properties including the elastic modulus (E), the shear modulus (G), and Poisson's ratio (v) from the three tests. However, the plate load test represents the near surface modulus, or the modulus within the bearing failure zone, and the unconfined test results returns the moduli for a free standing sample with no stresses. The seismic refraction test gives realistic estimation for the initial or small strain elastic moduli.

According to the interpreted soil parameters, the shear strength parameters have been estimated and can be used directly, or the given interrelations can be used (make sure if want to perform this analysis), or simply, the plate load test can be conducted and the results can be interpreted reliably according to the procedures followed in this report.

It is worth mentioning that the strength parameters either obtained from the UCS test or from the plate load test have been reduced considerably upon wetting conditions. The Unconfined strength has been reduced by a percent that ranged from 10% up to 50%. The plate load test has been reduced upon five-hour wetting cycle by more than 10% in some cases.

RECOMMENDATIONS

a) It is recommended that the shear strength parameters to be used by the practitioners to be within the provided ranges in this report
b) The deformability parameters are also to be within the provided ranges
c) The provided interrelations that was developed based on data availability of readily obtainable Marlparameters, for the both deformability and shear strength can be used for both bearing capacity and settlement estimation
d) For the case where the unconfined compressive strength test can be conducted, it is recommended to soak the samples until saturation
e) Plate Load Test is a representative sample when affordable, and it is recommended to perform the test after excavation reach the bearing strataand conducting prolonged wetting cycles to the test position.

ACKNOWLEDGEMENT

This research project has been supported by a generous grant from The University of Jordan / Deanship of Scientific research.

REFERENCES

Abd Elsamee W. N. 2013. An Experimental study on the effect of foundation Depth, Size and Shape on Subgrade Reaction of cohessionless soil. Engineering. 5, 785-795.

Adams M. T. and Collin J. G. 1997. Large model spread footing load tests on geosynthetic reinforced soil foundations. Journal of geotechnical and geo environmental engineering. 123(1): 66-72.

Akili W. and Torrance J. K. 1981. The development and geotechnical problems of sabkha, with preliminary experiments on the static penetration resistance of cemented sands. Quarterly Journal of Engineering Geology. 14(1): 59-73.

Al-Amoudi O. S. B., Khan K. and Al-Kahtani N. S. 2010. Stabilization of a Saudi calcareous Marl soil. Construction and Building Materials. 24(10): 1848-1854.

Al-Saigh N. H. and Al-Heety A. J. 2014. Seismic refraction tomography and MASW survey for geotechnical evaluation of soil for the teaching hospital project at Mosul University. Journal of Zankoy Sulaimani-Part A (JZS-A). 16(1): 1-13.

Alnuaim A., Hamid W. and Alshenawy A. 2019. Unconfined compressive strength and Young's modulus of Riyadh limestone. Electronic Journal of Geotechnical Engineering, 24, 707-717.

Amiri M., Dehghani M., Javadzadeh T. and Taheri S. 2022. Effects of lead contaminants on engineering properties of Iranian Marl soil from the microstructural perspective. Minerals Engineering. 176, 107310.

Anomohanran O. 2013. Seismic refraction method: A technique for determining the thickness of stratified substratum. American Journal of Applied Sciences. 10(8): 857-862.

Anyang M. Y., Atarigiya B. D., Ofori-Addo R. and Allotey N. K. 2018. Plate load test: getting it right. 49th Ghana Institution of Engineers (GhIE) Annual Conference, Ghana.

Arifuzzaman M. d., Najjar M., Mahmud M. N., Saiful Islam A. B. M., Khan I. and Ali M. M. 2017. Enhancing the properties of Marl soils for effective construction in Saudi Arabian region. Engineering Journal. 21(4): 111-126.

ASTM-D1194. 1994. Standard test method for bearing capacity of soil for static load and spread footings. In. West Conshohocken: ASTM International.

ASTM-D2938. 1995. Standard test method for unconfined compressive strength of intact rock core specimens. In. West Conshohocken.

Avci B. and Gurbuz A. 2018. Modulus of subgrade reaction that varies with magnitude of displacement of cohesionless soil. Arabian Journal of Geosciences. 11, 1-8.

Ayolabi E. A., Adeoti L., Oshinlaja N. A., Adeosun I. O. & Idowu O. I. 2009. Seismic refraction and resistivity studies of part of Igbogbo Township, south-west Nigeria. Journal Sci. Res. Dev. 11, 42-61.

Benyahia S., Boumezbeur A., Lamouri B. and Fagel N. 2020. Swelling properties and lime stabilization of N'Gaous expansive Marls, NE Algeria. Journal of African Earth Sciences.

Bery A. A. 2013. High resolution in seismic refraction tomography for environmental study. International Journal of Geosciences. 4, 792-796.

Birch F. 1961. The velocity of compressional waves in rocks to 10 kilobars: 2. Journal of Geophysical Research. 66(7): 2199-2224.

Bowles J. E. 1997. Foundation analysis and design (5 ed.). McGraw-Hill Book Co.

Briševac Z., Pollak D., Maričić A. and Vlahek A. 2021. Modulus of elasticity for grain-supported carbonates-determination and estimation for preliminary engineering purposes. Applied Sciences. 11(13): 6148.

Cichowicz, A., Birch, D., and Ogasawara, H. (2011). Multi-channel analysis of surface waves: inversion strategy. Proceedings of the Thirteenth International Conference on Civil, Structural and Environmental Engineering Computing, Stirlingshire, Scotland.

Diene, C. D., and Ndiaye, M. (2022). Design and application of a multichannel analysis surface waves acquisition system for the pavement layers investigation. Open Journal of Civil Engineering, 12(1).

Firoozi, A. A., Firoozi, A. A., and Baghini, M. S. (2017). A review of physical and chemical clayey. J Civ Eng Urban, 6(4), 64-71.

Ghanem F. K., Al Amoush H. and Al-Tarazi E. 2021. Geotechnical Engineering Evaluation of Superficial Deposits Utilizing Seismic Methods at Al al-Bayt University, Jordan. Iraqi Geological Journal. 54, 11-28.

Hodgkinson J. and Brown R. J. 2005. Refraction across an angular unconformity between nonparallel TI media. Geophysics. 70(2): D19-D28.

Hooshmand A., Aminfar M. H., Asghari E. and Ahmadi H. 2012. Mechanical and physical characterization of Tabriz Marls, Iran. Geotechnical and Geological Engineering. 30(1): 219-232.

Ige J. A. and Ajamu S. O. 2015. Unconfined compressive strength test of a fly ash stabilized sandy soil. International Journal of Latest Research in Engineering and Technology. 1(3): 1-11.

Jalal F. E., Mulk S., Memon S. A., Jamhiri B. and Naseem A. 2021. Strength, hydraulic, and microstructural characteristics of expansive soils incorporating marble dust and rice husk ash. Advances in Civil Engineering. 2021, 18.

Khalil M. H. and Hanafy S. M. 2008. Engineering applications of seismic refraction method: A field example at Wadi Wardan, Northeast Gulf of Suez, Sinai, Egypt. Journal of Applied Geophysics. 65, 132-141.

Khalil M. H. and Hanafy S. M. 2016. Geotechnical parameters from seismic measurements: Two field examples from Egypt and Saudi Arabia. Journal of Environmental and Engineering Geophysics. 21(1): 13-28.

Lamas F., Irigaray C. and Chacón J. 2002. Geotechnical characterization of carbonate Marls for the construction of impermeable dam cores. Engineering geology. 66, 283-294.

Lankston R. W. 1989. The seismic refraction method: A viable tool for mapping shallow targets into the 1990s. Geophysics. 54(12): 1535-1542.

Lin P.-S., Yang L.-W. and Juang C. H. 1998. Subgrade reaction and load-settlement characteristics of gravelly cobble deposits by plate-load tests. Canadian geotechnical journal. 35, 801-810.

Mahajan A. K., Sporry R. J., Champati Ray P. K., Ranjan R., Slob S. and Van W. C. 2007. Methodology for site-response studies using multi-channel analysis of surface wave technique in Dehradun city. Current science. 92(7).

Małkowski P., Ostrowski Ł. and Brodny J. 2018. Analysis of Young's modulus for Carboniferous sedimentary rocks and its relationship with uniaxial compressive strength using different methods of modulus determination. Journal of Sustainable Mining. 17, 145-157.

Milani S. J., Kaljahi E. A., Barzegari G. and Bonab M. H. 2017. Consolidation deformation of Baghmisheh Marls of Tabriz, Iran. Geomechanics and Engineering. 12, 561-577.

Nazir R., Momeni E., Armaghani D. J. and Amin M. F. M. 2013. Correlation between unconfined compressive strength and indirect tensile strength of limestone rock samples. Electron J Geotech Eng. 18(1): 1737-1746.

Park C. 2013. MASW for geotechnical site investigation. The Leading Edge. 32(6): 656-662.

Park C. B., Miller R. D., Xia J. and Ivanov J. 2007. Multichannel analysis of surface waves (MASW)-active and passive methods. The Leading Edge. 26(1): 60-64.

Salimi M., Kaljahi E. A. and Bonab M. H. 2018. Expansive soils characterizations and their destructive effects on Tabriz Northern Highway, Iran. GeoShanghai International Conference: Fundamentals of Soil Behaviours, Singapore.

Shaqour F. M., Jarrar G., Hencher S. and Kuisi M. 2008. Geotechnical and mineralogical characteristics of Marl deposits in Jordan. Environmental geology. 55(8): 1777-1783.

Vakili A. H., Salimi M. and Shamsi M. 2021. Application of the dynamic cone penetrometer test for determining the geotechnical characteristics of Marl soils treated by lime. Heliyon. 7.

Yong R. N. and Ouhadi V. R. 2007. Experimental study on instability of bases on natural and lime/cement-stabilized clayey soils. Applied clay science. 35(3-4): 238-249.